Proceedings of the
47th IEEE Conference on Decision and Control
Cancun, Mexico, Dec. 9-11, 2008

Feedback control of entanglement in a linear quantum network: A case study

Naoki Yamamoto*, Hendra I. Nurdin†, Matthew R. James† and Ian R. Petersen‡
* Department of Applied Physics and Physico-Informatics, Keio University, Yokohama 223-8522, Japan
Email: yamamoto@appi.keio.ac.jp
† Department of Engineering, Australian National University, Canberra ACT 0200, Australia
Email: {hendra.nurdin, matthew.james}@anu.edu.au
‡ School of Information Technology and Electrical Engineering,
University of New South Wales at the Australian Defence Force Academy, Canberra, ACT 2600, Australia
Email: i.petersen@adfa.edu.au

Abstract— **In this paper, we consider a linear quantum network composed of two distantly separated cavities that are connected via a one-way optical field. When one of the cavity is damped and the other is undamped, the overall cavity state obtains a large amount of entanglement in its quadratures. This entanglement however immediately decays and vanishes in a finite time. That is, entanglement sudden-death occurs. We show that the proportional measurement feedback method proposed by Wiseman can avoid this entanglement sudden-death, and further, enhance the entanglement. It is also shown that the entangled state under feedback control is robust against signal loss in a realistic detector, indicating the reliability of the proposed proportional feedback method in practical situations.**

I. Introduction

Reliable generation and distribution of *entanglement* in a quantum network is a central subject in quantum information technology [1], especially in quantum communication [2]–[5]. The biggest issue in such systems is the decay of entanglement due to *decoherence* effects that are inevitably introduced when node-channel or channel-environment interaction occurs. Entanglement distillation [6], [7] is a useful technique that restores such degraded entanglement. However, it sometimes happens that entanglement completely disappears in a finite time, which is called *entanglement sudden-death* [8], [9]. In this case, distillation techniques cannot recover the vanished entanglement.

On the other hand, feedback control can be used to modify the dynamical structure of a system and improve its performance, e.g., see [10]–[13]. Entanglement protection or generation is one of the most attractive applications of feedback [14]–[17]. In particular, two studies have demonstrated that a feedback controller effectively assists in the distribution of entanglement in a quantum network. One such result is by Mancini and Wiseman [18], where a proportional measurement feedback method [19], [20] is used to enhance the correlation of two bosonic modes that couple through a $\chi^{(2)}$ nonlinearity. (This control method is called direct measurement feedback in physics community.) The other such result is by Yanagisawa [21], where an estimation-based feedback controller is used to deterministically generate an entangled photon number state of two distantly separated cavities.

This paper follows a similar direction to [18] and [21]. That is, we also consider a problem of distributing entanglement in a quantum network using proportional feedback control. The quantum network being considered is depicted in Fig. 1: Two spatially separated cavities are connected via a one-way optical field, and the measurement results of the output of Cavity 2 are directly fed back to control both cavities. A more specific description will be given in Sections II-B and II-C, but here we note that the network model considered brings together the following three features that have been not simultaneously considered in previous work. First, the network contains models of realistic components; a realistic quantum channel in contact with an environment and a realistic homodyne detector with finite bandwidth [22]. A realistic model is of practical importance for real-time quantum feedback control. Second, we consider linear continuous-variable cavity models (i.e., we consider the quadratures of the cavity mode), similar to the case of [4], [5], [18]. Hence, the system differs from a discrete-variable system such as an atomic energy level [2], [3], or a photon number system description [21]. This setup is motivated by the recent rapid progress and deep understanding of continuous-variable systems in the quantum information regime [23]. Third, the cavities are spatially separated, and the interaction between them is simply mediated by an optical field, while in [18] two bosonic modes interact through a $\chi^{(2)}$ optical nonlinearity and thus the two modes are not spatially separated. The spatially separated case is the case of interest in applications such as quantum communication.

The contributions of this paper are as follows. First, we show that the network considered in this paper, which looks complicated, can be systematically captured and described using the theory of quantum cascade systems [24]–[27]. We then show that when the first cavity is undamped and the second cavity is damped, the cavity state obtains a large amount of entanglement, which, however, disappears in a finite time despite the continuous interaction between the cavities; i.e., entanglement sudden-death occurs. As mentioned above, no distillation technique can recover such a zero entanglement. Nevertheless, we show that proportional feedback control not only prevents entanglement sudden-death, but can also enhance the entanglement. Moreover, it will be shown that

978-1-4244-3124-3/08/$25.00 ©2008 IEEE

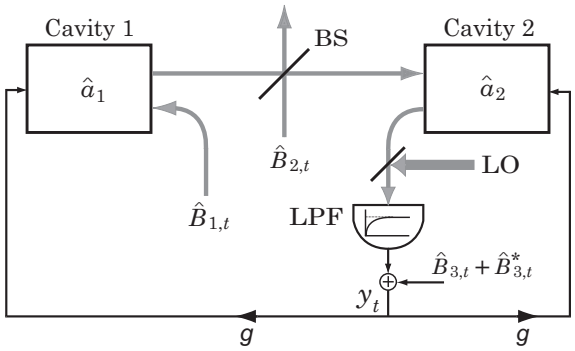

Fig. 1. Schematic of the network. Thick gray lines represent quantum optical fields, while thin black lines represent classical signals.

the entangled state under control is robust against signal loss in a realistic detector, implying the reliability of the proportional feedback method in practical situations.

Notation: For a matrix $A = (a_{ij})$, the symbols A^{T}, $A^\dagger$, and A^* represent its transpose, conjugate transpose, and elementwise complex conjugate of A, respectively. $\mathrm{Re}(A)$ and $\mathrm{Im}(A)$ denote the real and imaginary part of A, respectively. The matrix element a_{ij} can be an operator $\hat{a}_{ij}$; in this case, $\hat{a}_{ij}^*$ denotes its adjoint operator.

II. Model

A. General linear quantum systems

We consider a general linear continuous-variable system with N-degrees of freedoms. Let $\hat{\mathbf{x}}_i = (\hat{q}_i, \hat{p}_i)^{\mathsf{T}}$ be the standard quadrature pair of the i-th subsystem. It then follows from the canonical commutation relation $[\hat{q}_i, \hat{p}_j] = \hat{q}_i\hat{p}_j - \hat{p}_j\hat{q}_i = \mathrm{i}\delta_{ij}$ that the vector $\hat{\mathbf{x}} := (\hat{\mathbf{x}}_1^{\mathsf{T}}, \ldots, \hat{\mathbf{x}}_N^{\mathsf{T}})^{\mathsf{T}}$ satisfies

$$\hat{\mathbf{x}}\hat{\mathbf{x}}^{\mathsf{T}} - (\hat{\mathbf{x}}\hat{\mathbf{x}}^{\mathsf{T}})^{\mathsf{T}} = \mathrm{i}\Sigma_N = \mathrm{i}\bigoplus_{k=1}^{N}\Sigma, \quad \Sigma := \begin{bmatrix} 0 & 1 \\ -1 & 0 \end{bmatrix}.$$

Assume that the system contacts with M vacuum fields without scattering. Such an interaction is described by a unitary operator obeying the *Hudson-Parthasarathy equation* [28]:

$$d\hat{U}_t = \Big[\big(-\mathrm{i}\hat{H} - \frac{1}{2}\sum_{k=1}^{M}\hat{L}_k^*\hat{L}_k\big)dt + \sum_{k=1}^{M}\big(\hat{L}_k d\hat{B}_{k,t}^* - \hat{L}_k^* d\hat{B}_{k,t}\big)\Big]\hat{U}_t, \quad \hat{U}_0 = \hat{I}. \quad (1)$$

The operators $\hat{B}_{k,t}$ and $\hat{B}_{k,t}^*$ represent the quantum annihilation and creation processes on the k-th field, respectively. They are quantum analogues of classical Wiener processes; indeed, they satisfy $[d\hat{B}_{i,t}, d\hat{B}_{j,t}^*] = \delta_{ij}dt$. Let us choose $\hat{H} = \hat{H}^*$ and $\hat{L}_k$ as follows:

$$\hat{H} = \hat{\mathbf{x}}^{\mathsf{T}}G\hat{\mathbf{x}}/2, \quad \hat{L}_k = L_k^{\mathsf{T}}\hat{\mathbf{x}}, \quad (2)$$

where $G = G^{\mathsf{T}} \in \mathbb{R}^{2N\times 2N}$ and $L_k \in \mathbb{C}^{2N}$. The system variables obey the Heisenberg equation $\hat{\mathbf{x}}_t := (\ldots, \hat{U}_t^*\hat{q}_i\hat{U}_t, \hat{U}_t^*\hat{p}_i\hat{U}_t, \ldots)^{\mathsf{T}}$. We then obtain the following linear equation:

$$d\hat{\mathbf{x}}_t = A\hat{\mathbf{x}}_t dt + \mathrm{i}\Sigma_N[L^{\mathsf{T}}d\hat{\mathbf{B}}_t^* - L^\dagger d\hat{\mathbf{B}}_t], \quad (3)$$

where $L^{\mathsf{T}} := (L_1, \ldots, L_M) \in \mathbb{C}^{2N\times M}$, $A := \Sigma_N[G + \mathrm{Im}(L^\dagger L)]$, and $\hat{\mathbf{B}}_t := (\hat{B}_{1,t}, \ldots, \hat{B}_{M,t})^{\mathsf{T}}$. For details on the physical meaning of these abstract linear models, see, e.g., [39], [40]. It is easy to see that the first moment vector $\langle\hat{\mathbf{x}}_t\rangle := (\ldots, \langle\hat{U}_t^*\hat{q}_i\hat{U}_t\rangle, \langle\hat{U}_t^*\hat{p}_i\hat{U}_t\rangle, \ldots)^{\mathsf{T}}$, where $\langle\hat{x}\rangle := \mathrm{Tr}\,(\hat{\rho}\hat{x})$, satisfies the linear equation $d\langle\hat{\mathbf{x}}_t\rangle/dt = A\langle\hat{\mathbf{x}}_t\rangle$. Also, the covariance matrix $V_t = (\langle\hat{\mathbf{V}}_{ij}\rangle)$, where

$$\hat{\mathbf{V}} = \frac{1}{2}\Big[\Delta\hat{\mathbf{x}}_t\Delta\hat{\mathbf{x}}_t^{\mathsf{T}} + (\Delta\hat{\mathbf{x}}_t\Delta\hat{\mathbf{x}}_t^{\mathsf{T}})^{\mathsf{T}}\Big], \quad \Delta\hat{\mathbf{x}}_t := \hat{\mathbf{x}}_t - \langle\hat{\mathbf{x}}_t\rangle,$$

satisfies the following Lyapunov matrix differential equation:

$$dV_t/dt = AV_t + V_tA^{\mathsf{T}} + D. \quad (4)$$

Here, $D := \Sigma_N\mathrm{Re}(L^\dagger L)\Sigma_N^{\mathsf{T}}$. Suppose that the *state*, which is a quantum analogue to a classical probability density, is *Gaussian* [29], [30], [35] at $t = 0$. Then, from the linearity of the dynamics, the unconditional state is always Gaussian with mean $\langle\hat{\mathbf{x}}_t\rangle$ and covariance V_t. Note that the unconditional state corresponds to a classical probability density that describes a linear diffusion process.

B. The ideal network

Before describing the quantum network depicted in Fig. 1, let us consider the ideal situation where the optical field between the cavities is not in contact with any environment, and the homodyne detector is perfect. In this case, the system is the simple cascade of two cavities with a feedback loop. The entangled state of this ideal network will be compared to that of the realistic one for the purpose of clarifying how much the realistic parameters affect the system. Also, this ideal setup allows us to determine a reasonable control Hamiltonian (the vector f given below), as will be seen in Section III-B.

Each component of the network is described as follows. The optical vacuum field $\hat{B}_{1,t}$ comes into Cavity 1, and then, its output becomes the input of Cavity 2. We assume that, after some approximations, the i-th cavity-field interaction is represented by Eq. (1) with single field $(M = 1)$ and with the following operators:

$$\hat{H}_i = \hat{\mathbf{x}}_i^{\mathsf{T}}G_i\hat{\mathbf{x}}_i/2, \quad \hat{L}_{1,i} = \ell_i^{\mathsf{T}}\hat{\mathbf{x}}_i, \quad (i = 1, 2).$$

The subscript $(1, i)$ in $\hat{L}$ means the 1-st field and the i-th cavity. Also, $G_i = G_i^{\mathsf{T}} \in \mathbb{R}^{2\times 2}$ and $\ell_i \in \mathbb{C}^2$. The output of Cavity 2 is transformed to a classical signal y_t through an ideal homodyne detector. Suppose now that each cavity has an additional Hamiltonian of the form

$$\hat{H}_i^{\mathrm{fb}} = u_t\hat{F}_i = u_t f_i^{\mathsf{T}}\hat{\mathbf{x}}_i, \quad f_i \in \mathbb{R}^2, \quad (i = 1, 2),$$

where $u_t \in \mathbb{R}$ is the control input. Then, proportional measurement feedback $u_t = gy_t$ closes the loop by connecting the detector to the cavities. Here $g \in \mathbb{R}$ is the control gain. Note that we need a classical communication channel

in order to control Cavity 1; that is, a local operation via classical communication (LOCC) type control is performed.

For this network, we can easily determine the system matrices G and L_k in Eq. (2) that specify the whole dynamical equation. The derivation is based on the theory of quantum cascade systems [24]–[27] and is given in [31]. Then, from the definition, the A and D matrices in the Lyapunov equation (4) are readily obtained as follows:

$$A_{\rm id} = A_o + 2g\Sigma_2 f {\rm Re}(\ell)^{\mathsf T}, \tag{5}$$

$$D_{\rm id} = D_o + \Sigma_2\big[g^2 f f^{\mathsf T} - g{\rm Im}(\ell) f^{\mathsf T} - g f {\rm Im}(\ell)^{\mathsf T}\big]\Sigma_2^{\mathsf T}, \tag{6}$$

where $\ell = (\ell_1^{\mathsf T}, \ell_2^{\mathsf T})^{\mathsf T}$, $f = (f_1^{\mathsf T}, f_2^{\mathsf T})^{\mathsf T}$, and

$$A_o = \begin{bmatrix} A_1 & 0 \\ 2\Sigma{\rm Im}(\ell_2^*\ell_1^{\mathsf T}) & A_2 \end{bmatrix}, \quad D_o = \begin{bmatrix} D_1 & \star \\ \Sigma{\rm Re}(\ell_2^*\ell_1^{\mathsf T})\Sigma^{\mathsf T} & D_2 \end{bmatrix}. \tag{7}$$

Here, $A_i = \Sigma[G_i + {\rm Im}(\ell_i^*\ell_i^{\mathsf T})]$, $D_i = \Sigma{\rm Re}(\ell_i^*\ell_i^{\mathsf T})\Sigma^{\mathsf T}$, and $\star$ denotes the symmetric elements. Note that A_o and D_o are the system matrices of the network without feedback. Hence, the upper off-diagonal block matrix of A_o is zero, implying the one-way interaction of the cavities.

C. The realistic network

We are now in the position to describe a realistic network, which introduces the following two assumptions. First, the output of Cavity 1 is mixed with another vacuum field $\hat{B}_{2,t}$ through a beam splitter (BS) with transmittance α. This is a standard model of possible environmental effects on a long quantum channel. Second, the homodyne detector is not perfect and is described by the classical dynamics

$$d\xi_t = a_1\xi_t dt + a_2 dw_t, \quad dy_t = a_3\xi_t dt + dv_t, \quad a_i \in \mathbb{R}, \tag{8}$$

where w_t is an input stochastic process satisfying $\mathbf{E}[dw_t^2] = dt$ and v_t is an additional measurement noise satisfying $\mathbf{E}[dv_t^2] = a_4 dt$ ($a_4 > 0$). In particular, a typical low-pass filter (LPF) is realized by choosing a_i as

$$a_1 = -1/\tau, \quad a_2 = 1/\tau, \quad a_3 = 1,$$

where $\tau > 0$ is the time-constant. We now note that the detector (8) can be represented as a quantum system with two fields $w_t = \hat{B}'_{1,t} + \hat{B}'^*_{1,t}$ and $v_t = \hat{B}_{3,t} + \hat{B}^*_{3,t}$, where $\hat{B}'_{1,t}$ is the output of Cavity 2. Indeed, from [27], Eq. (1) with $M = 2$ and with the operators

$$\hat{H}_3 = \frac{a_1}{2}(\hat{q}_3\hat{p}_3 + \hat{p}_3\hat{q}_3), \quad \hat{L}_{1,3} = -{\rm i}a_2\hat{p}_3, \quad \hat{L}_{3,3} = \frac{a_3}{2a_4}\hat{q}_3$$

leads to a linear equation of the form (8), where $\hat{U}_t^*\hat{q}_3\hat{U}_t$ plays the same role of ξ_t.

Consequently, the network is composed of two cavities, a beam splitter, a detector, and a controller, with three optical vacuum fields. (Note that the beam splitter with local oscillator (LO) shown in Fig. 1 is a part of the detector.) To systematically obtain the overall system matrices G and L_k in Eq. (2) of this complicated network, we again use the theory of quantum cascade systems [24]–[27]. The procedure is given in [31]. We then obtain the matrices A and D in Eq. (4) as follows:

$$A_{\rm re} = \begin{bmatrix} A_1 & 0 & ga_3\Sigma f_1 \\ 2\alpha\Sigma{\rm Im}(\ell_2^*\ell_1^{\mathsf T}) & A_2 & ga_3\Sigma f_2 \\ 2\alpha a_2{\rm Re}(\ell_1)^{\mathsf T} & 2a_2{\rm Re}(\ell_2)^{\mathsf T} & a_1 \end{bmatrix}, \tag{9}$$

$$D_{\rm re} = \begin{bmatrix} D_1 & \star & \star \\ \alpha\Sigma{\rm Re}(\ell_2^*\ell_1^{\mathsf T})\Sigma^{\mathsf T} & D_2 & \star \\ -\alpha a_2{\rm Im}(\ell_1)^{\mathsf T}\Sigma^{\mathsf T} & -a_2{\rm Im}(\ell_2)^{\mathsf T}\Sigma^{\mathsf T} & a_2^2 \end{bmatrix} + g^2 a_4 \begin{bmatrix} \Sigma f_1 f_1^{\mathsf T}\Sigma^{\mathsf T} & \star & 0 \\ \Sigma f_2 f_1^{\mathsf T}\Sigma^{\mathsf T} & \Sigma f_2 f_2^{\mathsf T}\Sigma^{\mathsf T} & 0 \\ 0 & 0 & 0 \end{bmatrix}. \tag{10}$$

III. Entanglement control

In this section, we study the entanglement of the cavity state for the ideal network. Since the state is Gaussian, its entanglement is completely characterized by the covariance matrix [29], [30]. In our case, the covariance matrix to be evaluated is obtained from Eq. (4) with the coefficient matrices $A_{\rm id}$ and $D_{\rm id}$ in Eqs. (5) and (6). Let the matrices V_i be defined by the 2×2 block matrix decomposition of V as follows:

$$V = \begin{bmatrix} V_1 & V_2 \\ V_2^{\mathsf T} & V_3 \end{bmatrix}.$$

Then, the following *logarithmic negativity* [32] can be used as a reasonable measure of Gaussian entanglement:

$$E_{\mathcal N} = \max\{0, \ -\log(\sqrt{2}\nu)\}, \tag{11}$$

where $\log x$ denotes the natural logarithm of x,

$$\nu := \sqrt{\tilde{\Delta} - \sqrt{\tilde{\Delta}^2 - 4{\rm det}(V)}}, \tag{12}$$

$$\tilde{\Delta} := {\rm det}(V_1) + {\rm det}(V_3) - 2{\rm det}(V_2).$$

The logarithmic negativity $E_{\mathcal N}$ divides the state space into two regions: (i) the separable region, corresponding to $E_{\mathcal N} = 0$, and (ii) the entangled region, within which $E_{\mathcal N} > 0$. Thus phenomena of entanglement creation and destruction can be understood simply in terms of movement of the system between these two regions.

A. Entanglement sudden-death

Here we study the uncontrolled network; i.e., $g = 0$.

We compute $E_{\mathcal N}$ for two situations. First, consider the case where both cavities have the same quadratic Hamiltonian and are damped as a result of the field-cavity interaction, that is,

$$G_1 = G_2 = {\rm diag}\{m, 1\}, \quad \ell_1 = \ell_2 = \sqrt{\kappa}(1, \ {\rm i})^{\mathsf T},$$

where $m > 0$ and $\kappa > 0$. This type of quadratic Hamiltonian can be implemented in a cavity system following the scheme of the *degenerate parametric amplification* [26]. In this case, $A_{\rm id}$ is a *stable matrix*, and Eq. (4) has a unique steady state solution (see e.g., [33]). Now assume that at $t = 0$, the cavity is in the separable state satisfying $V_0 = 2I$. When the optical field is switched on, the cavity modes couple after a finite time (i.e., the "entanglement sudden-birth" [34] occurs), and a steady entangled state is generated as seen from the dotted

line in Fig. 2 (a). However, in this case, the entanglement is very small ($E_{\mathcal{N}} \approx 0.21$).

This result can be understood by examining the trajectory of the parameter $(\tilde{\Delta}, \det(V))$. In Fig. 3, the colored region with contour lines represents the set of parameters where a general two-mode Gaussian state is entangled, i.e., $E_{\mathcal{N}} > 0$, while the white region corresponds to separable states; i.e., $E_{\mathcal{N}} = 0$. The trajectory, denoted by $\mathcal{T}_{\rm dam}$, evolves toward the steady entangled state that is located far from the area with large $E_{\mathcal{N}}$ (the right bottom area in Fig. 3). This is likely because each cavity has a strong tendency to transit into the vacuum state due to the damping. Indeed, when the cavity is in the separable vacuum state $|0\rangle|0\rangle$, the corresponding covariance matrix satisfies $(\tilde{\Delta}, \det(V)) = (0.5, 0.0625)$, which is very close to the equilibrium point of $\mathcal{T}_{\rm dam}$. Moreover, Fig. 2 (b) shows that the *purity* (for a discussion of physical meanings of the purity, see e.g. [35]) of the steady Gaussian state $\hat{\rho}$,

$$P := \mathrm{Tr}\,(\hat{\rho}^2) = \frac{1}{4\sqrt{\det(V)}} \in (0, 1], \qquad (13)$$

approaches $P \approx 0.8$ as $t \to \infty$. This also suggests that the steady state is close to the separable vacuum state.

The above observation motivates us to try a dispersive field-cavity interaction, which results in a phase shift of the output field [10], [36], [37]. For a practical method to implement this kind of coupling in a cavity system, see [31]. In this case, the cavity is not damped, and thus, it does not have a tendency to move toward the vacuum state. In particular, we assume that only the first cavity has such an interaction; i.e.,

$$\ell_1 = (\sqrt{\kappa},\ 0)^{\mathsf{T}}, \quad \ell_2 = \sqrt{\kappa}(1,\ \mathrm{i})^{\mathsf{T}}.$$

We then find that $A_{\rm id}$ is not a stable matrix, and the Lyapunov equation (4) need not have a steady state solution as $t \to \infty$. Fig. 3 shows that the corresponding trajectory, denoted by $\mathcal{T}_{\rm dis}$, evolves far from the separable initial state and reaches the area with large $E_{\mathcal{N}}$. This figure also shows how both the entanglement and purity decreases as time goes on and $\mathcal{T}_{\rm dis}$ escapes from the region of entangled states at $t = 6.2$.

Finally, we remark that, if we exchange the order of the interactions, i.e., $\ell_1 = \sqrt{\kappa}(1,\ \mathrm{i})^{\mathsf{T}}$ and $\ell_2 = (\sqrt{\kappa},\ 0)^{\mathsf{T}}$, the corresponding trajectory remains within the region of separable states, i.e., $E_{\mathcal{N}} = 0$ for all $t > 0$. The situation is much the same even when each cavity interacts with the field in a dispersive way.

B. Feedback control

We first discuss how to determine the coefficient vector $f = (f_1^{\mathsf{T}}, f_2^{\mathsf{T}})^{\mathsf{T}}$ that realizes high-quality entanglement control. Fortunately, in the ideal case, we can explicitly find such an f. The idea was originally provided by Wiseman and Doherty in [38], but here we apply the idea in a slightly different manner.

Assume that $g = 1$. Then, Eq. (4) with coefficient matrices $A_{\rm id}$ and $D_{\rm id}$ in Eqs. (5) and (6) can be rewritten as

$$dV_t/dt = \mathcal{R}(V_t) + \Sigma_2(f - f_t)(f - f_t)^{\mathsf{T}}\Sigma_2^{\mathsf{T}}, \qquad (14)$$

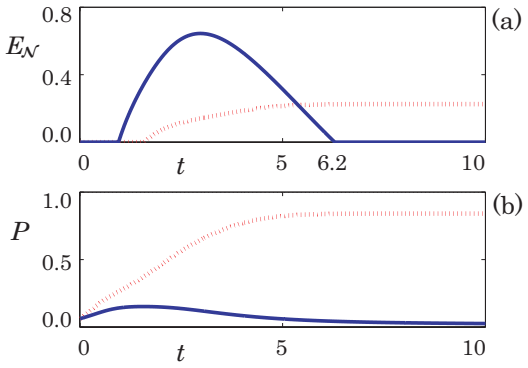

Fig. 2. Time-dependence of the logarithmic negativity (a) and the purity (b) of the overall cavity state without feedback control. The solid and dotted lines correspond to the dispersive-damped and damped-damped cases, respectively. The parameters are $m = 0.2$ and $\kappa = 1$.

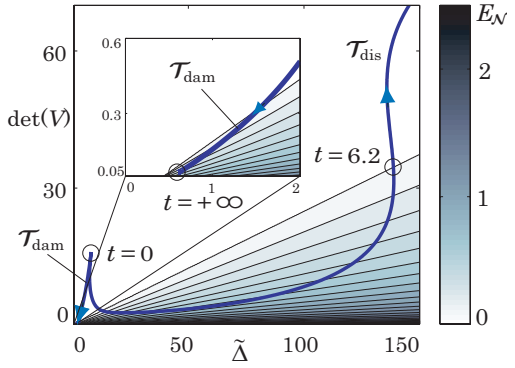

Fig. 3. Trajectories of the parameter $(\tilde{\Delta}, \det(V))$ without feedback control. $\mathcal{T}_{\rm dam}$ and $\mathcal{T}_{\rm dis}$ correspond to the damped-damped and dispersive-damped cases, respectively. We set $V_0 = 2I$ at $t = 0$, from which $\tilde{\Delta} = 8$ and $\det(V_0) = 16$ follow.

where $f_t := 2\Sigma_2 V_t \mathrm{Re}(\ell) + \mathrm{Im}(\ell)$ and

$$\mathcal{R}(V) := A_o V + V A_o^{\mathsf{T}} + D_o - \Big[2V\mathrm{Re}(\ell) - \Sigma_2\mathrm{Im}(\ell)\Big]\Big[2V\mathrm{Re}(\ell) - \Sigma_2\mathrm{Im}(\ell)\Big]^{\mathsf{T}}.$$

We now recall from Fig. 2 (b) that entanglement sudden-death occurs simultaneously with a decrease of the purity (13). This suggests that preventing a decrease of purity may also prevent entanglement sudden-death. However, we should point out that it is not apparent that this will always be the case and the relationship between loss of purity and entanglement sudden-death needs to be studied further. Therefore, a simple control strategy that we try here is to find a feedback controller that prevents an increase of $\det(V_t)$ in order to keep the purity high. As the second term of the right-hand side of Eq. (14) is always non-negative, it is then reasonable to choose the time-variant coefficient vector $f = f_t$. Of course, this intuitive argument does not always allow us to conclude that $\det(V_t)$ takes its minimum value. However, it is known that the algebraic Riccati equation $\mathcal{R}(V) = 0$ has a solution satisfying $\det(V) = 1/16$, which implies that the maximum purity $P = 1$ is achieved; e.g., see [38]. Now assume that Eq. (14) has a unique steady

solution V_∞ for a constant f. Then, by taking the time-invariant coefficient vector

$$\bar{f} := 2\Sigma_2 V_\infty \mathrm{Re}(\ell) + \mathrm{Im}(\ell), \quad \mathcal{R}(V_\infty) = 0, \tag{15}$$

we obtain the same desirable result, $\det(V_\infty) = 1/16$.

We now consider proportional feedback control with the coefficient vector (15). Let us begin with the case where the first cavity-field interaction occurs dispersively. For this system, it is expected from Fig. 3 that the trajectory $\mathcal{T}_{\rm dis}$ can be modified and stabilized via feedback so that it has an equilibrium point in the area where $E_\mathcal{N}$ is large. That this is indeed true is shown below. When the parameters are given by $m = 0.2$ and $\kappa = 1$, we find that $\bar{f} = (0.1212, 2.2196, -0.3163, -3.2277)^{\mathsf{T}}$ from (15). Fig. 5 illustrates that the controlled trajectory, denoted by $\mathcal{T}^{\rm c}_{\rm dis}$, indeed shows the convergence that we had hoped for. The entanglement and the purity of the steady cavity state are shown in Fig. 4. While $\bar{f}$ is determined with fixed $g = 1$, we consider variations in g to gain understanding about its effect on the control system. When control is not used ($g = 0$), the pair of dispersive and damped cavities does not settle down to a steady state as seen in Section III-A, and we find that $E_\mathcal{N} \to 0$ as $t \to \infty$. On the other hand, even with the small-gain feedback controller, the system becomes stable and has a unique steady state with nonzero entanglement. Remarkably, when $g = 1$, the entanglement of the steady state ($E_\mathcal{N} \approx 2.2$) improves upon the maximum value of $E_\mathcal{N}$ of the uncontrolled state ($E_\mathcal{N} \approx 0.65$) shown in Fig. 2 (a). Hence we see that proportional feedback not only prevents entanglement sudden-death, but can also enhance the entanglement.

Feedback can also improve the entanglement of a system where both cavities are damped, but it is still very small as seen from the dotted line in Fig. 4 (a). (The coefficient vector (15) in this case is calculated to be $\bar{f} = (0.0629, 0.1525, 0.2479, -0.5830)$.) To understand this phenomenon, we recall that the uncontrolled trajectory $\mathcal{T}_{\rm dam}$ has an equilibrium point that is located far from the area with large $E_\mathcal{N}$. Hence, it should be hard to drastically modify this trajectory such that it could reach that area. It is actually observed in Fig. 5 that the controlled trajectory $\mathcal{T}^{\rm c}_{\rm dam}$ shows almost the same time-evolution as the autonomous one $\mathcal{T}_{\rm dam}$.

The above results suggest that strong stability of the autonomous system sometimes makes it difficult for the state to transit into a desirable entangled target.

IV. A REALISTIC CONTROL SCENARIO

Finally, we return to the original setup of the network. That is, the quantum channel is in contact with an environment, and the homodyne detector is replaced by a realistic LPF with finite bandwidth. The purpose here is to study the impacts of these realistic components on the entanglement of the cavity state. The covariance matrix of the cavity state corresponds to the left-upper 4×4 submatrix of V_t that is the solution of Eq. (4) with $A_{\rm re}$ and $D_{\rm re}$ given in Eqs. (9) and (10). Note that the cavity state is the reduced one with the detector mode traced out. We here focus only on the network

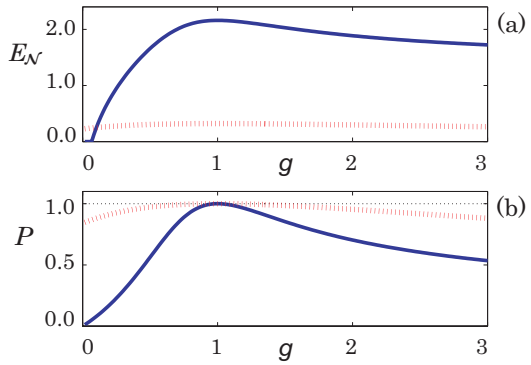

Fig. 4. The logarithmic negativity (a) and the purity (b) of the steady cavity state with feedback control. g is the control gain. The solid and dotted lines correspond to the dispersive-damped and damped-damped cases, respectively. The parameters are $m = 0.2$ and $\kappa = 1$.

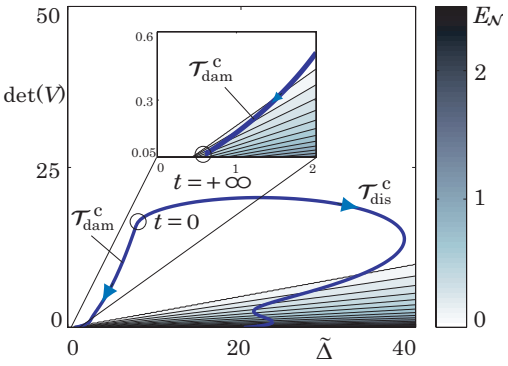

Fig. 5. Trajectories of the parameters $(\tilde{\Delta}, \det(V))$ with feedback control. $\mathcal{T}^{\rm c}_{\rm dam}$ and $\mathcal{T}^{\rm c}_{\rm dis}$ correspond to the damped-damped and dispersive-damped cases, respectively. The initial state is the same as before: $V_0 = 2I$.

where the first cavity interacts with the field dispersively. For the control Hamiltonian, we use the same coefficient vector $\bar{f} = (0.1212, 2.2196, -0.3163, -3.2277)^{\mathsf{T}}$. It should be noted that, in this realistic case, we cannot follow the discussion in Section III-B to obtain a reasonable coefficient vector f.

First, consider Fig. 6 (a). This shows some plots of $E_\mathcal{N}$ with the time-constant τ changing between $0.01 \le \tau \le 0.6$ and with the fixed transmittance $\alpha = 1$ (i.e., no loss in the channel). The most upper line almost coincides with the ideal one shown in Fig. 4 (a). That is, the entanglement in the realistic situation continuously converges to the ideal one as $\tau \to 0$. We also observe that the degradation of $E_\mathcal{N}$ is small with respect to τ. Since the detector is regarded as a component of the controller, these results imply that the realistic proportional feedback is robust against signal loss in the LPF. In other words, proportional feedback control is reliable even in this realistic situation.

On the other hand, Fig. 6 (b) plots $E_\mathcal{N}$ for some values of the channel loss $\beta := 1 - \alpha$ with fixed $\tau = 0.01$. We find that $E_\mathcal{N}$ converges to the ideal one as $\beta \to 0$, similar to the above case. However, in this case, $E_\mathcal{N}$ rapidly decreases with respect to β. Even for the very small loss $\beta = 0.01$, a visible degradation occurs. Moreover, when $\beta = 0.1$,

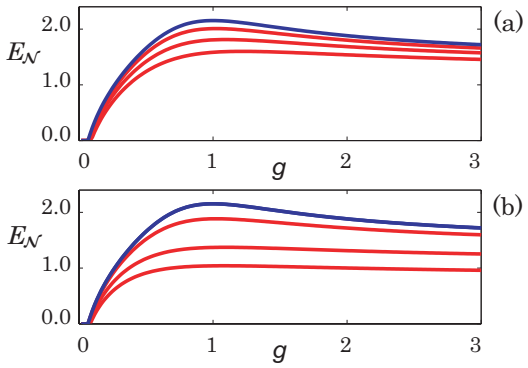

Fig. 6. The logarithmic negativity of the steady cavity state with feedback control. g is the control gain. (a) From the top downwards, the lines correspond to $\tau = 0.01, 0.2, 0.4, 0.6$, while $\alpha = 1$. (b) From the top downwards, the lines correspond to $\alpha = 1, 0.99, 0.95, 0.90$, while $\tau = 0.01$. In both cases, the LPF noise is small; $a_4 = 0.01$. The parameters are $m = 0.2$ and $\kappa = 1$.

which still means we have a high-quality quantum channel, $E_{\mathcal{N}}$ decreases less than half of the ideal one. That is, the entanglement is fragile to realistic channel loss.

The above results are reasonable because the channel loss directly reflects the decrease of interaction strength, while the finite bandwidth of LPF simply implies loss of a classical signal. Hence the former should be a critical factor for entanglement generation.

V. Conclusion

The contributions of this paper are summarized as follows. First, it was shown that, when the first cavity is undamped and the second one is damped, the overall cavity state obtains a significant amount of entanglement, which however disappears in a finite time. Then, we have shown that proportional measurement feedback can avoid this entanglement sudden-death, and further, enhances the entanglement. Moreover, it was shown that the proportional feedback controller is reliable under the influence of signal loss in a realistic detector, although imperfection in the quantum channel is a critical issue that largely degrades the achieved entanglement.

References

[1] M. A. Nielsen and I. L. Chuang, *Quantum Computation and Quantum Information*, (Cambridge University Press, Cambridge, 2000).
[2] J. I. Cirac, P. Zoller, J. H. Kimble, and H. Mabuchi, Quantum state transfer and entanglement distribution among distant nodes in a quantum network, Phys. Rev. Lett. 78, 3221 (1997).
[3] S. J. van Enk, J. I. Cirac, and P. Zoller, Ideal quantum-communication over noisy channels: a quantum optical implementation, Phys. Rev. Lett. 78, 4293 (1997).
[4] A. S. Parkins and H. J. Kimble, Quantum state transfer between motion and light, J. Opt. B: Quantum Semiclass. Opt. 1, 496 (1999).
[5] A. S. Parkins and H. J. Kimble, Position-momentum Einstein-Podolsky-Rosen state of distantly separated trapped atoms, Phys. Rev. A 61, 052104 (2000).
[6] C. H. Bennett, G. Brassard, S. Popescu, B. Schumacher, J. A. Smolin, and W. K. Wootters, Purification of Noisy Entanglement and Faithful Teleportation via Noisy Channels, Phys. Rev. Lett. 76, 722 (1996).
[7] C. H. Bennett, D. P. DiVincenzo, J. A. Smolin, and W. K. Wootters, Mixed-state entanglement and quantum error correction, Phys. Rev. A 54, 3824 (1996).
[8] T. Yu and J. H. Eberly, Finite-time disentanglement via spontaneous emission, Phys. Rev. Lett. 93, 140404 (2004).
[9] J. H. Eberly and T. Yu, The end of an entanglement, Science, 316, 27 (2007).
[10] A. C. Doherty and K. Jacobs, Feedback control of quantum systems using continuous state estimation, Phys. Rev. A 60, 2700 (1999).
[11] L. Thomsen, S. Mancini, and H. M. Wiseman, Continuous quantum nondemolition feedback and unconditional atomic spin squeezing, J. Phys. B, 35, 4937 (2002).
[12] C. Ahn, H. M. Wiseman, and G. J. Milburn, Quantum error correction for continuously detected errors, Phys. Rev. A 67, 052310 (2003).
[13] L. M. Bouten, R. van Handel, and M. R. James, A discrete invitation to quantum filtering and feedback control, to appear in SIAM Review, arXiv: math/0606118 (2006).
[14] J. Wang, H. M. Wiseman, and G. J. Milburn, Dynamical creation of entanglement by homodyne-mediated feedback, Phys. Rev. A 71, 042309 (2005).
[15] A. R. R. Carvalho and J. J. Hope, Stabilizing entanglement by quantum-jump-based feedback, Phys. Rev. A 76, 010301(R) (2007).
[16] M. Mirrahimi and R. van Handel, Stabilizing feedback controls for quantum systems, *SIAM J. Control Optim.* 46, 445-467 (2007).
[17] N. Yamamoto, K. Tsumura, and S. Hara, Feedback control of quantum entanglement in a two-spin system, *Automatica* 43, 981-992 (2007).
[18] S. Mancini and H. M. Wiseman, Optimal control of entanglement via quantum feedback, Phys. Rev. A 75, 012330 (2007).
[19] H. M. Wiseman and G. J. Milburn, Quantum theory of optical feedback via homodyne detection, Phys. Rev. Lett. 70, 548 (1993).
[20] H. M. Wiseman, Quantum theory of continuous feedback, Phys. Rev. A 49, 2133 (1994).
[21] M. Yanagisawa, Quantum feedback control for deterministic entanglement photon generation, Phys. Rev. Lett. 97, 190201 (2006).
[22] P. Warszawski, H. M. Wiseman, and H. Mabuchi, Quantum trajectories for realistic detection, Phys. Rev. A 65, 023802 (2002).
[23] S. L. Braunstein and P. van Loock, Quantum information with continuous variables, Rev. Mod. Phys. 77, 513 (2005).
[24] H. J. Carmichael, *An open system approach to quantum optics*, Springer, Berlin (1993).
[25] H. J. Carmichael, Quantum trajectory theory for cascaded open systems, Phys. Rev. Lett. 70, 2273 (1993).
[26] C. W. Gardiner and P. Zoller, *Quantum Noise*, Springer, Berlin (2000).
[27] J. Gough and M. R. James, The series product and its application to quantum feedforward and feedback networks, arXiv: 0707.0048 (2007).
[28] R. L. Hudson and K. R. Parthasarathy, Quantum Ito's formula and stochastic evolution, Commun. Math. Phys. 93, 301 (1984).
[29] L. M. Duan, G. Giedke, J. I. Cirac, and P. Zoller, Inseparability criterion for continuous variable systems, Phys. Rev. Lett. 84, 2722 (2000).
[30] R. Simon, Peres-Horodecki separability criterion for continuous variable systems, Phys. Rev. Lett. 84, 2726 (2000).
[31] N. Yamamoto, H. I. Nurdin, M. R. James, and I. R. Petersen, Avoiding entanglement sudden-death via measurement feedback control in a quantum network, arXiv: 0806.4754 (2008).
[32] G. Vidal and R. F. Werner, Computable measure of entanglement, Phys. Rev. A 65, 032314 (2002).
[33] K. Zhou, J. Doyle, and K. Glover, *Robust and Optimal Control*, Prentice Hall, NJ (1996).
[34] Z. Ficek and R. Tanas, Delayed sudden-birth of entanglement, Phys. Rev. A 77, 054301 (2008).
[35] M. G. A. Paris, F. Illuminati, A. Serafini, and S. DeSiena, Purity of Gaussian states: Measurement scheme and time evolution in noisy channel, Phys. Rev. A 68, 012314 (2003).
[36] G. J. Milburn, Classical and quantum conditional statistical dynamics, Quantum Semiclass. Opt. 8, 269 (1996).
[37] H. M. Wiseman and G. J. Milburn, Quantum theory of field-quadrature measurements, Phys. Rev. A 47, 642 (1993).
[38] H. M. Wiseman and A. C. Doherty, Optimal unravellings for feedback control in linear quantum systems, Phys. Rev. Lett. 94, 070405 (2005).
[39] H. I. Nurdin, M. R. James, and A. C. Doherty, Network synthesis of linear dynamical quantum stochastic systems, arXiv:0806.4448 (2008).
[40] M. R. James, H. I. Nurdin, and I. R. Petersen, to appear in IEEE Trans. Automat. Contr., arXiv:quant-ph/0703150 (2007).